communications biology

A Nature Portfolio journal

Article

https://doi.org/10.1038/s42003-025-07859-6

Arthropod autophagy molecules facilitate *Anaplasma phagocytophilum* infection of *Ixodes scapularis* tick cells

Check for updates

Jeremy W. Turck, Hameeda Sultana & Girish Neelakanta

Ixodes scapularis ticks transmit several medically important pathogens including *Anaplasma phagocytophilum* to humans and animals. In this study, we provide evidence that *A. phagocytophilum* modulates autophagy molecules for its survival in tick cells. qRT-PCR analysis revealed that *A. phagocytophilum* infection results in the upregulation of tyrosine phosphatase, *shp-2*, and serine/threonine-protein kinase, *mTOR*, in ticks and tick cells. RNAi-mediated knockdown of *shp-2* or functional blocking with SHP-2 inhibitor resulted in significantly increased bacterial burden and reduced phospho-mTOR levels in *A. phagocytophilum*-infected tick cells. In addition, treatment of *A. phagocytophilum*-infected tick cells with rapamycin (mTOR inhibitor) resulted in significantly increased bacterial burden and reduced phospho-mTOR levels. Furthermore, expression of autophagy molecules such as *atg14* and *ulk1* were noted to be upregulated in both *A. phagocytophilum*-infected unfed ticks and tick cells. RNAi-mediated silencing of *atg14* or *ulk1* affected bacterial growth in tick cells. Collectively, these results not only indicate distinct host and pathogen responses in tick-*A. phagocytophilum* interactions but also suggest that this bacterium modulates autophagy molecules for its survival in ticks.

In the United States, *Ixodes scapularis and Ixodes pacificus* are the predominant vectors that transmit *Anaplasma phagocytophilum*, the agent of human granulocytic anaplasmosis, to humans and animals[1–3]. *A. phagocytophilum* enters the tick vector when these arthropods take a blood meal from an infected reservoir host[1–4]. The developmental life stages of these ticks involve eggs, larvae, nymphs, and adults. The larvae take a blood meal and molt into nymphs[5,6]. If these larvae acquire an infectious blood meal containing *A. phagocytophilum*, they molt into infected nymphs[5,6]. *A. phagocytophilum* is transmitted to humans and animals upon a bite from an infected nymph[5,6]. After taking a blood meal, nymphs molt into either male or female adult ticks. Adult female ticks take a blood meal, mate with male ticks, and lay eggs. In nature, this cycle continues. However, *A. phagocytophilum* cannot undergo transovarial transmission in these ticks. Adult ticks could also transmit *A. phagocytophilum* if uninfected nymphs took an infectious blood meal and molt into adults[3].

A. phagocytophilum is an obligate intracellular gram-negative coccoid bacterium that colonizes neutrophils in the vertebrate host and salivary glands in the *I. scapularis* tick vector[7–9]. When *A. phagocytophilum* invades a host cell, it forms a host-derived vacuole known as a morulae[3,8,10]. The bacteria will grow and multiply in the morulae and later will exit from the morula and the host cell to spread to the neighboring host cells[3,8,10]. *A. phagocytophilum* can survive in the mammalian host cell by modulating several cellular processes including cytoskeleton remodeling, manipulating the defense response by epigenetic silencing, autophagy, decreasing the NADPH oxidase, and delaying apoptosis[3,11–15]. In ticks, *A. phagocytophilum* modulates several cellular processes for its acquisition, replication, survival, and transmission[16–29].

Intracellular signaling inside a host cell is initiated and terminated with enzymatic proteins called kinases and phosphatases[30]. Kinases will induce an activation or deactivation of a protein through phosphorylation, and a phosphatase will do the same function through the dephosphorylation of a protein or a complex[30]. *A. phagocytophilum* induces phosphorylation of several host proteins such as ROCK1, PAK, and actin for its survival and infection in mammalian and tick cells[21,31]. In addition, it has been reported that phosphorylation of *A. phagocytophilum* protein AnkA by host Abl-1 tyrosine kinase is important for its infection in mammalian cells[32]. Recently, we reported that *A. phagocytophilum* induces expression of Src tyrosine kinase and p38 MAPK for its survival in tick cells[18,23]. Treatment with Src or p38 MAPK dsRNAs or inhibitors affected *A. phagocytophilum* growth and replication in ticks and tick cells[18,23]. These studies indicate that kinases and

Department of Biomedical and Diagnostic Sciences, College of Veterinary Medicine, University of Tennessee, Knoxville, TN, USA.
e-mail: gneelaka@utk.edu

phosphatases are important for *A. phagocytophilum* survival in both mammalian and tick cells.

A. phagocytophilum activates phosphoinositide 3-kinase (PI3K) for its survival in ticks and tick cells[21]. Studies have elucidated that SH-2 domain-containing protein SHP-2 acts upstream to PI3K and modulates the PI3K signaling pathway[33,34]. SHP-2 is a tyrosine phosphatase that localizes near the intracellular surface of the cell[35,36]. PI3K is involved in the conversion of phosphatidylinositol 4,5-biphosphate (PI4, 5P2, or PIP2) into phosphatidylinositol 3,4,5-triphosphate (PI3, 4, $5P_3$, or PIP3)[33]. This conversion leads to the recruitment of phosphoinositide-dependent kinase 1 (PDK1) followed by AKT phosphorylation and activation of the mammalian target of rapamycin (mTOR)[33,34,36,37]. Autophagy is the process of self-degradation, and this process is balanced through the activity of mTOR[37,38]. The autophagy mechanism involves multiple steps including initiation, maturation, and termination of the autophagosome formation[37,38]. Autophagosome is a double-membrane vesicle and several molecules such as ATG13, ULK1, ATG14, ATG101, and Beclin-1 participate in the formation of this vesicle[37,38]. mTOR complex 1 (mTORC1) is the protein complex that is responsible for the inhibition of autophagosome formation[38]. mTORC1 regulates the autophagosome activity in a cell by interacting with autophagy-related proteins that are responsible for initiation, maturation, and termination of the autophagosome[37,38].

A. phagocytophilum effector protein AnkA recruits SHP-1 phosphatase upon phosphorylation[39]. This phenomenon is important for *A. phagocytophilum* infection in mammalian cells[39]. In addition, a study has reported that *A. phagocytophilum* effector protein Ats1 interacts with beclin-1 to recruit autophagosome for its growth in mammalian cells[15]. In mammalian cells, *A. phagocytophilum* prevents host-derived vacuoles from fusing with lysosome[40]. Several autophagy-related markers were noted to be localized on the *A. phagocytophilum*-containing vacuole[40]. These studies indicate that *A. phagocytophilum* subverts autophagy for its survival in mammalian cells. While much is known on the role of SHP phosphatases, mTOR, and autophagy pathway upon *A. phagocytophilum* infection in mammalian cells very little is known from the vector side. In this study, we provide evidence that *A. phagocytophilum* infection modulates the expression of SHP-2 and mTOR proteins in tick cells. In addition, we noted that inhibition of mTOR or RNAi-mediated-silencing of autophagy genes favors *A. phagocytophilum* infection in tick cells.

Results

Comparison of *Ixodes scapularis* SHP-2 tyrosine phosphatase to insect and mammalian orthologs

Ixodes scapularis ticks encode SHP-2 ortholog in their genome. We amplified the *shp-2* tyrosine phosphatase transcripts in ticks (GeneBank acc. No. XP_029830587) (Supplementary Fig. 1). QRT-PCR was used to amplify the (164 bp) product from cDNA prepared from total RNA of *I. scapularis* unfed nymphs (Supplementary Fig. 1). ClustalW alignment of *I. scapularis* SHP-2 amino acid sequence showed 53% identity with *Drosophila melanogaster* (GeneBank Acc. No. NP_477131.1) and 66% identity with *Aedes aegypti* (GeneBank acc. no. XP_021705063.1), *Mus musculus* (GeneBank Acc. No. NP_035332.1) and *Homo sapiens* (GeneBank acc. no. XP_054228694.1) SHP-2 orthologs (Supplementary Figs. 2 and 3A, B). The domain analysis of the *I. scapularis* SHP-2 protein revealed the presence of two SH-2 domains, a PTP-type protein phosphatase domain, and a tyrosine-specific domain (Supplementary Fig. 3C). The active site for *I. scapularis* SHP-2 tyrosine phosphatase is tyrosine residue 449. The phylogenetic tree analysis revealed that *I. scapularis* SHP-2 forms a separate clade when compared to the other analyzed insect and mammalian orthologs (Supplementary Fig. 3D). Human and mouse SHP-2 orthologs fall within one clade and *Drosophila melanogaster* and *Aedes aegypti* SHP-2 orthologs formed a different clade (Supplementary Fig. 3D). Furthermore, post-translational modification analysis revealed four *N*-glycosylation sites, seven *N*-myristoylation site, eleven Casein kinase II, and eleven protein kinase C sites (Supplementary Fig. 4A). In addition, we noted that SHP-2 orthologs from *D. melanogaster*, *A. aegypti, M. musculus* and *H. sapiens* also contained several of *N*-glycosylation sites, *N*-myristoylation site, Casein kinase II, and protein kinase C sites (Supplementary Fig. 4B–E). Collectively, these results reveal that even though tick SHP-2 forms a divergent clade, the functional domains and types of posttranslational modification sites were noted to be similar to the mammalian orthologs.

Expression of *shp-2* is variable in different developmental stages of *I. scapularis* ticks

We first analyzed the expression of *shp-2* transcripts in all the different life cycle stages of *I. scapularis* ticks. QRT-PCR analysis showed that there were significantly ($P < 0.05$) higher levels of *shp-2* transcripts in larvae when compared to nymph and adult male ticks (Fig. 1A). There were also significantly ($P < 0.05$) higher levels of *shp-2* transcripts in adult female ticks when compared to nymph and adult male ticks (Fig. 1A). No significant differences were observed in the *shp-2* transcript levels between larvae and female ticks or between nymphs and male ticks (Fig. 1A). The significant increase in *shp-2* expression suggests an important role for this molecule in larvae and adult female life stages of this vector.

A. phagocytophilum upregulates the expression of *shp-2* in unfed nymphs and in ISE6 tick cells

The role of SHP-2 in *I. scapularis*-*A. phagocytophilum* has not been studied. We first analyzed the expression of SHP-2 RNA and protein levels upon *A. phagocytophilum* infection in the tick vector. QRT-PCR results showed a significant ($P < 0.05$) increase in *shp-2* transcript levels in *A. phagocytophilum*-infected tick cells at tested time points of days 1 and 3 post-infection (p.i.) compared to the levels noted in uninfected control (Fig. 1B, C). In addition, we noted a significant ($P < 0.05$) increase in *shp-2* transcript levels in *A. phagocytophilum*-infected unfed nymphs when compared to the levels noted in uninfected controls (Fig. 1D). However, we did not observe any significant differences in the expression of *shp-2* transcripts in *A. phagocytophilum*-infected ticks either during feeding (Fig. 1E) or after feeding (Fig. 1F) when compared to the levels noted in the respective uninfected control groups (Fig. 1E, F). In addition, we did not observe any significant difference in the *shp-2* transcript levels during transmission of *A. phagocytophilum* from infected ticks to the naïve murine host when compared to the levels noted in uninfected ticks (Supplementary Fig. 5A). Immunoblotting performed with commercially available antibody against a vertebrate SHP-2 showed increased levels of arthropod SHP-2 in *A. phagocytophilum*-infected unfed nymphal ticks when compared to the levels noted in uninfected control (Fig. 1G and Supplementary Fig. 5B). The Ponceau-S-stained image served as a loading control image for the protein amounts that were used in the immunoblot analysis (Fig. 1G). Collectively, these results show that *A. phagocytophilum* upregulates SHP-2 in unfed nymphs and in tick cells.

RNAi-mediated silencing and functional inhibition of arthropod SHP-2 increases *A. phagocytophilum* burden in tick cells

The upregulation of SHP-2 in ticks and tick cells suggests an important role for this molecule in *A. phagocytophilum*-tick interactions. To further evaluate the role of SHP-2, we performed RNAi-mediated silencing analysis in tick cells. We amplified the *shp-2* fragment (329 bp) and cloned it into the pL4440 vector to generate *shp-2*-dsRNA. Similarly, multiple cloning site region in the pL4440 vector was considered for the generation of mock-dsRNA. Tick cells were treated with *shp*-2 or mock-dsRNA followed by *A. phagocytophilum* infection. QRT-PCR analysis revealed significant ($P < 0.05$) lower levels of *shp-2* transcripts in *shp-2*-dsRNA-treated *A. phagocytophilum*-infected tick cells compared to the levels noted in mock-treated control at 24 h p.i., (Fig. 2A). Interestingly, we noted a significant ($P < 0.05$) increase in *A. phagocytophilum* burden in *shp-2*-dsRNA-treated tick cells when compared to the bacterial burden noted in mock-dsRNA-treated control (Fig. 2B). Furthermore, we performed in vitro studies with a PTP type 11 SHP-2 inhibitor. Tick cells were treated with a 25 μM (final concentration) dose of the SHP-2 inhibitor and an equivalent amount of DMSO as mock control. We did not observe any morphological differences

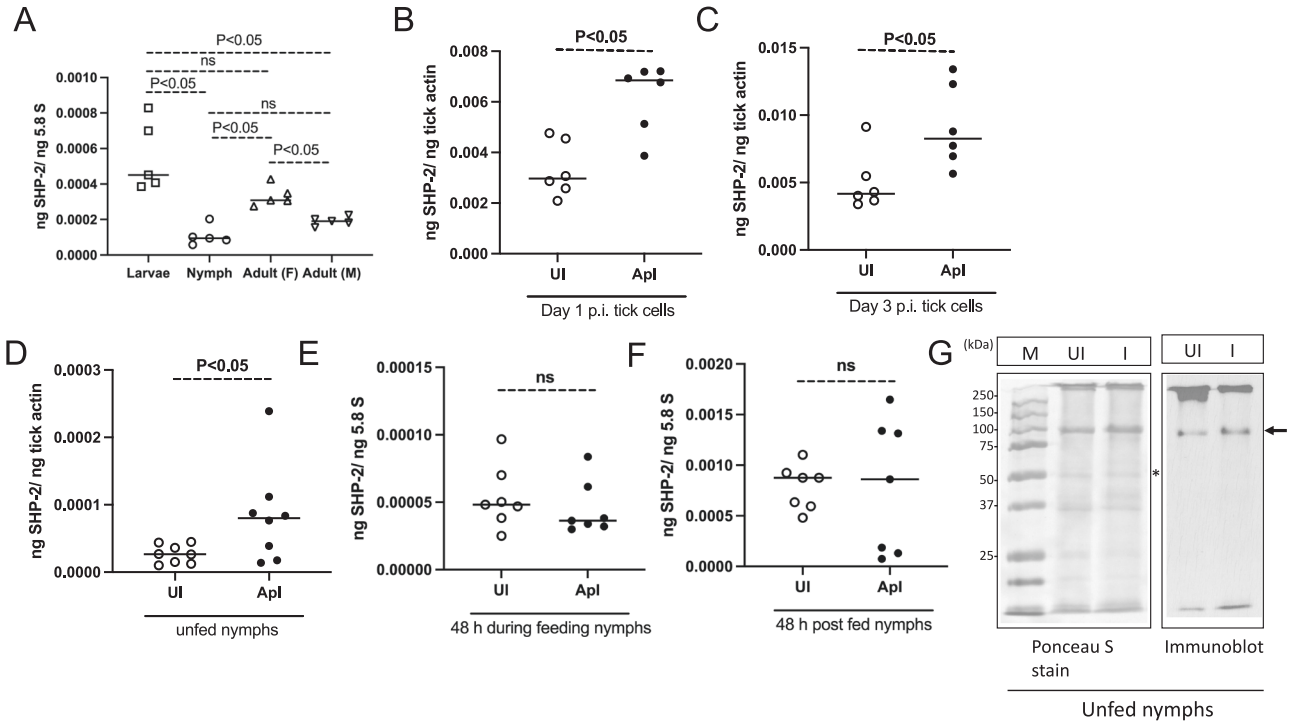

Fig. 1 | *Ixodes scapularis shp-2* transcript levels in ticks and tick cells. A QRT-PCR analysis showing the expression of *I. scapularis shp-2* transcripts at different developmental stages (larvae, nymphs, female, and male) of ticks. Each dot for larvae samples corresponds to data from a pool of about ten ticks, and each dot for nymphs and adults represents data from one tick. The *shp-2* transcript levels were normalized to 5.8S ribosomal RNA levels. QRT-PCR analysis showing *shp-2* transcripts at day 1 (**B**) or at day 3 (**C**) post-infection (p.i.) in uninfected or *A. phagocytophilum*-infected tick cells. Each dot represents data from samples collected from one culture well. The mRNA levels of *shp-2* were normalized to tick beta-actin mRNA. **D** QRT-PCR analysis showing *shp-2* transcript levels in unfed (**D**), 48 h during feeding (**E**), and 48 h post-feeding (repleted) uninfected (UI) or *A. phagocytophilum*-infected (ApI) ticks. For **B**–**F**, open circles represent data from uninfected (UI), and closed circles represent data from *A. phagocytophilum*-infected (ApI) tick cells (**B**, **C**) or ticks (**D**–**F**). In **E, F** *shp-2* transcript levels were normalized to 5.8S rRNA levels. *P* values for panel (**A**) from one-way ANOVA and (**B**–**F**) from non-paired *t*-test are shown. ns indicates not significant. **G** Immunoblotting analysis of SHP-2 protein amounts in uninfected (UI) or *A. phagocytophilum*-infected unfed nymphs is shown. The Ponceau-S-stained image serves as a loading control image. The asterisk indicates the band considered for normalization in densitometric analysis. The arrow indicates tick SHP-2 protein with a size of around 90 kDa. M indicates a marker in kDa. The marker sizes are shown on the left side of the Ponceau-S-stained image.

between tick cells treated with mock or SHP-2 inhibitor following *A. phagocytophilum*-infection (Supplementary Fig. 6A, B). QRT-PCR analysis revealed no significant differences in the *shp-2* transcripts upon treatment of *A. phagocytophilum*-infected tick cells with SHP-2 inhibitor in comparison to the levels noted in mock controls at 24 h p.i. (Fig. 2C). However, we noted a significant ($P < 0.05$) increase in *A. phagocytophilum burden* in SHP-2 inhibitor-treated tick cells when compared to the bacterial burden noted in mock-treated controls (Fig. 2D). These results indicate that genetic knockdown of *shp-2* expression or functional inhibition of SHP-2 protein facilitates *A. phagocytophilum* infection in tick cells.

Comparison of *I. scapularis* mammalian target of rapamycin (mTOR) to insect and mammalian orthologs

The upregulation of SHP-2 phosphatase in *A. phagocytophilum*-infected tick cells prompted us to delineate the downstream singling in this cascade. SHP-2 is reported to activate the mTOR pathway in the mammalian cells[33]. We, therefore combed the genome of *I. scapularis* and identified a mammalian ortholog of mTOR (GeneBank Acc. No. XP_042146895). The mTOR is a kinase that was initially identified in mammals[37,38]. The role of mTOR in *I. scapularis* has not been studied. QRT-PCR was used to amplify the *mTOR* transcript product (252 bp) from cDNA prepared from total RNA of *I. scapularis* unfed nymphs (Supplementary Fig. 7). ClustalW alignment of *I. scapularis* mTOR amino acid sequence showed a 56% identity with *D. melanogaster* mTOR (GeneBank Acc. No. NP_001260427), 58% identity with *A. aegypti* mTOR (GeneBank acc. no. AAR97336.1), 64% identity with *M. musculus* mTOR (GeneBank Acc. No. NP_064393.2) and 64% identify with *H. sapiens* mTOR (GeneBank Acc. No. NP_001373429.1) (Supplementary Figs. 8A, B and 9A, B). Domain analysis of *I. scapularis* SHP-2 revealed the presence of a FAT domain, a PI3K/PI4K catalytic domain, and a FATC domain (Supplementary Fig. 9C). A phylogenetic tree analysis of mTOR revealed that *I. scapularis* mTOR formed a separate clade from other analyzed SHP-2 orthologs. (Supplementary Fig. 9D). The human and mouse mTORs form one clade and mTORs from *D. melanogaster* and *A. aegypti* form a different clade. Post-translational modification analysis of *I. scapularis* mTOR revealed two amidation sites, five cAMP phosphorylation sites, seven N-glycosylation sites, 28 *N*-myristoylation sites, 32 Casein kinase II sites, and 30 protein kinase C sites (Supplementary Fig. 10A). In addition, we noted that mTOR orthologs from *D. melanogaster*, *A. aegypti, M. musculus* and *H. sapiens* also contained several of *N*-glycosylation, *N*-myristoylation, amidation, cAMP phosphorylation, Casein kinase II, and protein kinase C sites (Supplementary Fig. 10B–E). Overall, a high degree of percent identity in amino acid sequence and conservation of domains and types of posttranslational modification sites in *I. scapularis* mTOR suggests a similar role for tick molecule in various signaling pathways like its mammalian counterpart.

Expression of *mTOR* in different developmental stages of *I. scapularis*

We then analyzed whether mTOR is expressed in all developmental stages of *I. scapularis* ticks. QRT-PCR analysis revealed significantly ($P < 0.05$) higher levels of *mTOR* transcripts in larvae when compared to nymph and adult male ticks (Fig. 3A). No significant difference in *mTOR* transcripts was

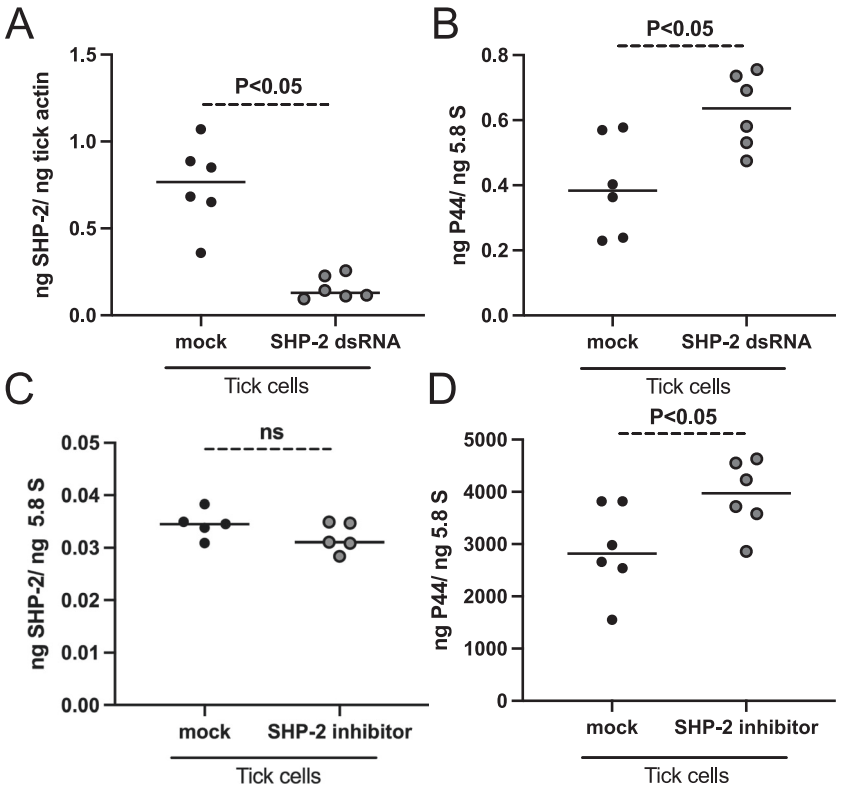

Fig. 2 | Knockdown or inhibition of arthropod SHP-2 increases *A. phagocytophilum* loads in tick cells. A QRT-PCR analysis showing *shp-2* transcript levels (**A**, **C**) or bacterial burden (**B**, **D**) at 24 h p.i. in mock-dsRNA-treated (**A**, **B**) or *shp-2*-dsRNA-treated (**A**, **B**) or mock solution (DMSO)-treated (**C**, **D**) or SHP-2-inhibitor-treated (**C**, **D**) *A. phagocytophilum*-infected tick cells. Black circles represent data from mock-dsRNA-treated or mock-solution-treated, and the gray circles represent data from *shp-2*-dsRNA-treated or SHP-2 inhibitor-treated *A. phagocytophilum*-infected tick cells. In all panels, each circle represents data for samples collected from one individual cell culture plate well. The *shp-2* mRNA levels and *p44* DNA levels were normalized to 5.8S rRNA levels. The *P* value from the non-paired *t*-test is shown. ns indicates not significant.

evident between nymphal and adult ticks. These data show that *mTOR* transcripts are highly expressed in larvae when compared to other developmental stages of ticks.

A. phagocytophilum upregulates the expression of *mTOR* in unfed nymphs and in tick cells

As SHP-2 activates mTOR, we reasoned whether *A. phagocytophilum* infection has any impact on mTOR expression. QRT-PCR analysis revealed significant upregulation of *mTOR* transcripts in *A. phagocytophilum*-infected tick cells at both tested time points of 1 and 3 p.i. when compared to the levels noted in uninfected tick cells (Fig. 3B, C). In addition, we noted that *mTOR* transcripts were significantly upregulated in *A. phagocytophilum*-infected unfed nymphal ticks compared to the levels noted in uninfected unfed controls (Fig. 3D). However, we did not observe any significant differences ($P > 0.05$) in the *mTOR* transcripts in *A. phagocytophilum*-infected ticks during feeding (Fig. 3E) or after feeding (Fig. 3F) when compared to the levels noted in respective fed uninfected ticks (Fig. 3E, F).

Functional inhibition of mTOR increases *A. phagocytophilum* loads in tick cells

Furthermore, in vitro studies were performed with rapamycin, an inhibitor of mTOR. No morphological differences were noted between tick cells treated with mock or rapamycin following *A. phagocytophilum*-infection (Supplementary Fig. 11A, B). QRT-PCR analysis revealed significantly ($P < 0.05$) reduced levels of mTOR transcripts in rapamycin-treated *A. phagocytophilum*-infected tick cells when compared to the levels noted in mock-treated controls (Fig. 4A). In addition, QRT-PCR analysis revealed significantly ($P < 0.05$) increased *A. phagocytophilum* burden in rapamycin-treated tick cells when compared to the bacterial burden noted in mock-treated control (Fig. 4B). We then performed immunoblotting analysis to determine levels of activated mTOR (phospho-mTOR). Immunoblotting analysis showed a decrease in the phospho-mTOR levels in rapamycin-treated *A. phagocytophilum*-infected tick cells when compared to the levels noted in mock-treated control (Fig. 4C and Supplementary Fig. 12A). In addition, we also noted a reduced phospho-mTOR levels in *shp-2*-dsRNA-treated (Fig. 4D and Supplementary Fig. 12B) and SHP-2 inhibitor-treated (Fig. 4E and Supplementary Fig. 12C) *A. phagocytophilum*-infected tick cells compared to the levels noted in respective mock-treated controls (Fig. 4D, E). Collectively, these results not only demonstrate that SHP-2 acts upstream of mTOR and is important in the activation of the water molecule but also show that functional inhibition of mTOR increases *A. phagocytophilum* burden in tick cells.

A. phagocytophilum upregulates the expression of several autophagy markers in unfed nymphs and ISE6 tick cells

It has been reported that mTOR inhibits autophagy induction, nucleation at the endoplasmic reticulum, autophagosome elongation, and autophagosome maturation[38]. We, therefore, reasoned to analyze the expression of autophagy markers in tick and tick cells upon *A. phagocytophilum* infection. QRT-PCR analysis revealed that autophagy markers that are responsible for autophagosome formation and maturation including Atg13, ULK1, Atg14, beclin-1, and p300 were all significantly ($P < 0.05$) upregulated in *A. phagocytophilum*-infected unfed nymphal ticks compared to the levels noted in uninfected controls (Fig. 5A–E). In tick cells, *atg13* expression did not show any significant differences at both tested time points of day 1 and day 3 p.i. (Fig. 6A, F). The *ulk1* expression was significantly ($P < 0.05$) upregulated in *A. phagocytophilum*-infected tick cells compared to the expression noted in uninfected control at day 1 and 3 p.i. (Fig. 6B, G). At day 1 p.i., the expression of *atg14* was not affected (Fig. 6C) but at day 3 p.i. the expression of this gene was significantly upregulated in *A. phagocytophilum*-infected tick cells compared to the expression noted in uninfected control (Fig. 6H). The expression of beclin-1 and p300 was unaltered in *A. phagocytophilum*-infected tick cells compared to the expression noted in uninfected controls at both day 1 (Fig. 6D, E) and day 3 post-infection time points (Fig. 6I, J).

Rapamycin treatment has no effects on the expression of several autophagy markers in tick cells

We then tested whether rapamycin treatment affects the expression of autophagy markers. QRT-PCR analysis revealed that expression of *atg13* (Fig. 7A), *ulk1* (Fig. 7B), *atg14* (Fig. 7C), and *beclin-1* (Fig. 7D) was unaltered

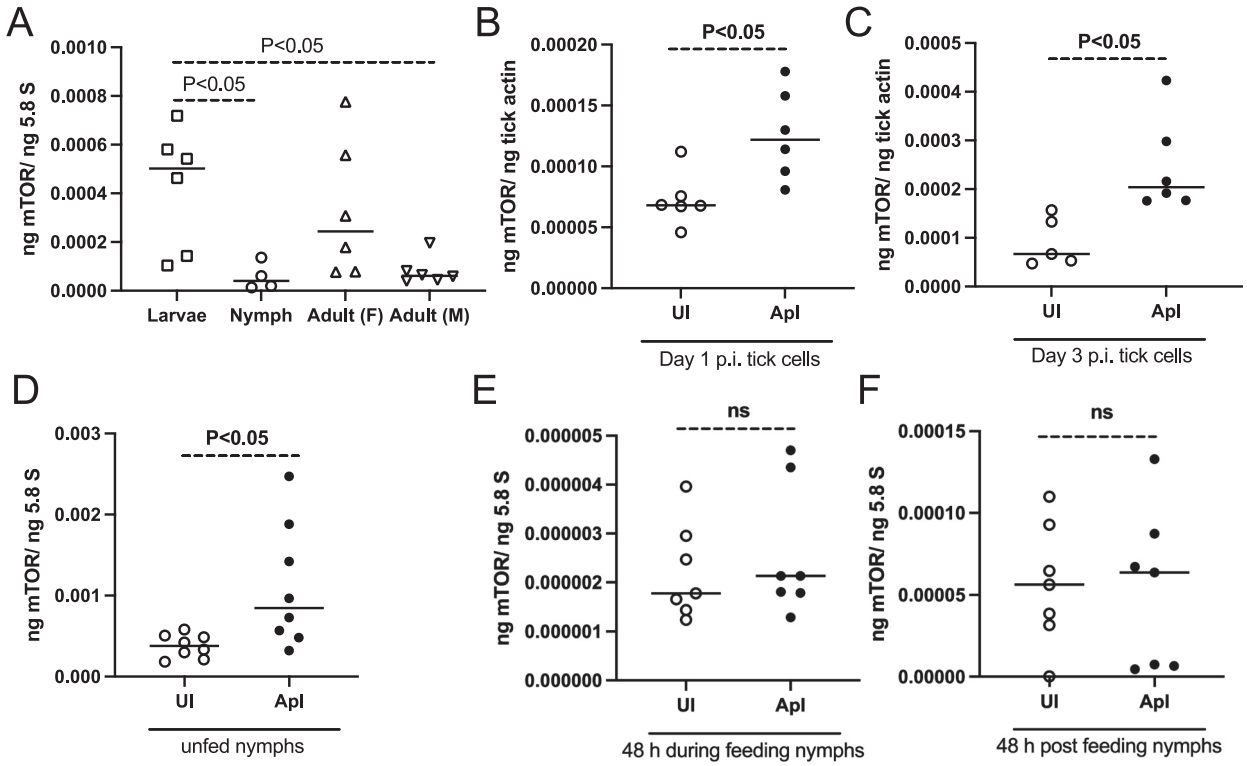

Fig. 3 | *Ixodes scapularis mTOR* transcript levels in tick and tick cells. A QRT-PCR analysis showing levels of *I. scapularis mTOR* transcripts at different developmental stages (larvae, nymphs, female, and male) of ticks. For larvae samples, each dot corresponds to data from a pool of about ten ticks. For nymphs and adult samples, each dot represents data from one tick. The *mTOR* transcript levels were normalized to 5.8S rRNA levels. QRT-PCR analysis showing *mTOR* transcripts at days 1 (**B**) or day 3 (**C**) post-infection (p.i.) in uninfected or *A. phagocytophilum*-infected tick cells. Each dot represents data from samples collected from one culture well. The mRNA levels of *mTOR* were normalized to tick beta-actin mRNA levels. **D** QRT-PCR analysis showing expression of *mTOR* transcripts in unfed (**D**), 48 h during feeding (**E**), and 48 h post-feeding (repleted) uninfected (UI) or *A. phagocytophilum*-infected (ApI) ticks. **B**–**F** Open circles represent data from uninfected (UI) and closed circles represent data from *A. phagocytophilum*-infected (ApI) tick cells (**B**, **C**) or ticks (**D**–**F**). In **E**, **F** *mTOR* transcript levels were normalized to 5.8S rRNA levels. *P* values for panel A from one-way ANOVA and panels B-F from non-paired *t*-test are shown. ns indicates not significant.

in *A. phagocytophilum*-infected ticks cells treated with rapamycin compared to the expression levels noted in cells treated with mock control (Fig. 7A–D). A similar observation was noted in uninfected tick cells (Fig. 7E–H). These results suggest that blocking mTOR function with rapamycin treatment has no effects on the transcript levels of *atg13*, *ulk1*, *atg14*, and *beclin-1*.

RNAi-mediated silencing of *atg14* or *ulk1* expression affects *A. phagocytophilum* loads in tick cells

Upregulation of *atg14* and *ulk1* expression in ticks and tick cells upon *A. phagocytophilum* infection prompted us to test whether RNAi-mediated silencing of the expression of these genes has any impact on bacterial growth. Tick cells were treated with *atg14*- or *ulk1*- or mock-dsRNA followed by *A. phagocytophilum* infection. QRT-PCR analysis revealed that *atg14* transcripts were significantly ($P < 0.05$) less in *atg14*-dsRNA-treated *A. phagocytophilum*-infected tick cells compared to the levels noted in the mock-treated control group (Fig. 8A). In addition, we noted significantly ($P < 0.05$) decreased levels of bacterial burden in *atg14*-dsRNA-treated *A. phagocytophilum*-infected tick cells compared to the burden noted in mock-treated control (Fig. 8B). Similarly, *ulk1* transcripts (Fig. 8C) and bacterial burden (Fig. 8D) were significantly ($P < 0.05$) reduced in *ulk1*-dsRNA-treated *A. phagocytophilum*-infected tick cells compared to the levels noted in mock-treated control. Collectively, these results not only indicate the upregulation of autophagy genes upon *A. phagocytophilum* infection in tick cells is independent of SHP-2-mTOR signaling but also shows that ATG14 and ULK1 are important for bacterial survival in these cells.

Discussion

The eukaryotic kinases and phosphatases are key molecules in mediating host-pathogen interactions[41]. In addition, bacterial pathogens deliver their kinases and phosphatases to alter host signaling[42]. These bacterial enzymes facilitate adhesion, virulence, replication, and survival in the host cells[41,42]. *A. phagocytophilum* also modulates kinases and phosphatases for its survival in mammalian and tick cells[21,23,31,39]. In this study, we provide new evidence that *A. phagocytophilum* infection of tick cells modulates SHP-2 phosphatase and its downstream molecule mTOR signaling for its survival. In addition, our study indicates that autophagy molecules such as ATG14 and ULK1 are important for *A. phagocytophilum* infection of tick cells.

Bioinformatic analysis revealed a high degree of amino acid sequence conservation of tick SHP-2 and mTOR with their mammalian counterparts. We noted more than 65% identity in the amino acid sequence of tick proteins with their mammalian orthologs. The presence of functional domains such as two SH-2 domains in SHP-2 and PI3K/PIK4 catalytic domain in tick mTOR suggests a high degree of conservation in their functions like their mammalian counterparts. Based on the amino acid length (GeneBank acc. no. XP_029830587.1), the tick SHP-2 protein molecular mass should be around 85 kDa. However, we noted an intense band around 90 kDa size. The increase in the band size could be due to potential phosphorylation on the tick SHP-2 protein. SHP-2 and mTOR are key players in growth, metabolism, and diseases[36,37]. The observation of

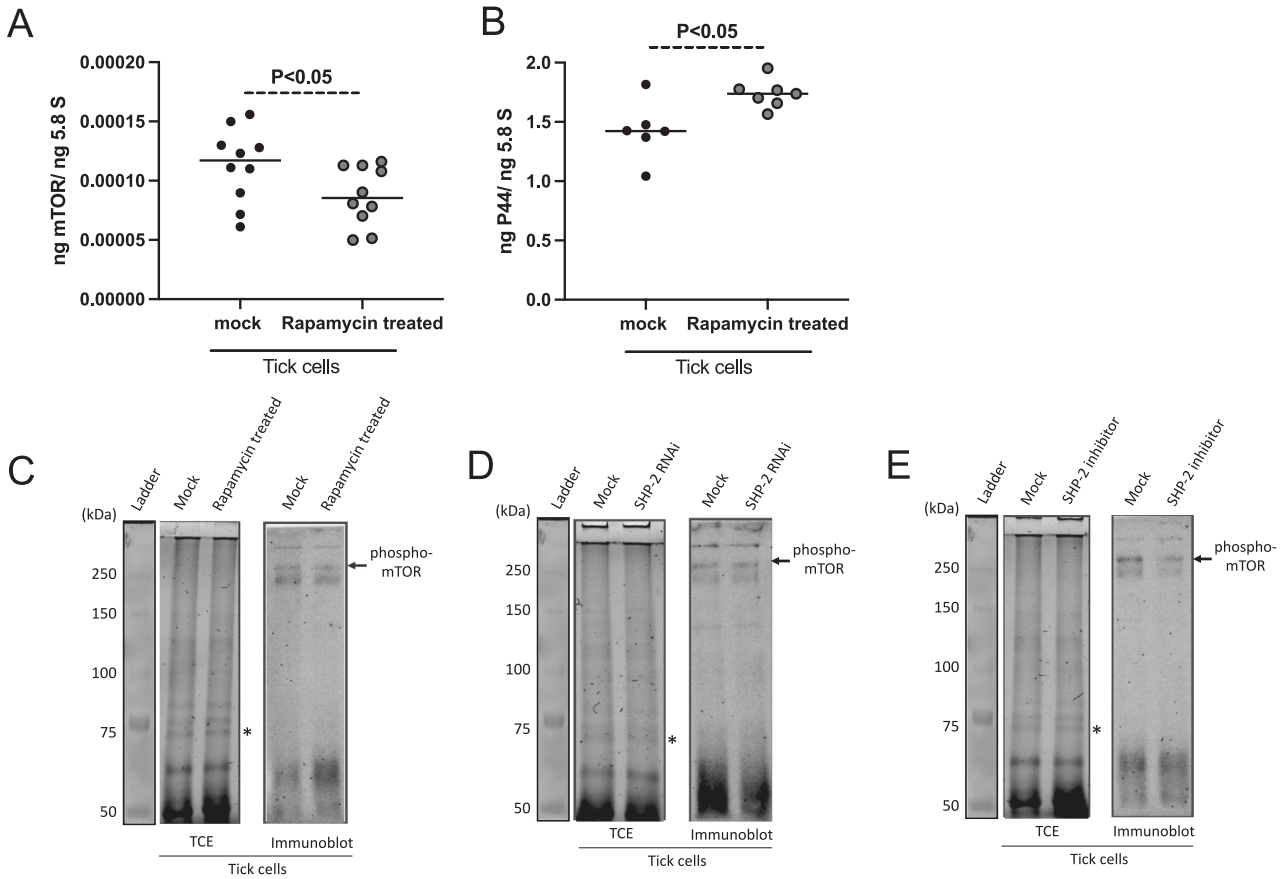

Fig. 4 | Rapamycin treatment increases *A. phagocytophilum* burden in tick cells. QRT-PCR analysis showing mTOR transcripts (**A**) and bacterial burden (**B**) in mock (DMSO) or rapamycin-treated *A. phagocytophilum*-infected tick cells. Each dot represents data from one independent culture plate well. The mRNA levels of mTOR and *p44* DNA levels were normalized to 5.8S rRNA levels. *P* value from the non-paired Student's *t*-test is shown. Immunoblot analysis showing phospho-mTOR levels in mock- or rapamycin-treated (**C**) or mock-dsRNA- or shp-2-dsRNA-treated (**D**) or mock- or SHP-inhibitor-treated (**E**) *A. phagocytophilum*-infected tick cells. For **C**, **D**, and **E**, the phospho-mTOR protein is shown with the black arrow at approximately 289 kDa position. All tick cell samples were infected with *A. phagocytophilum* and were collected at 24 h post-infection. TCE gel image serves as a loading control image. The asterisk indicates the band considered for normalization in densitometric analysis. Protein sizes in kDa are shown on the left side of the TCE gel image.

increased SHP-2 and mTOR transcripts in larval stages of ticks and in female ticks indicates their role in arthropod growth and development.

The up-regulation of SHP-2 upon *A. phagocytophilum* infection could be a host response to limit the infection. The observation of increased bacterial burden in *shp-2*-dsRNA-treated or SHP-2 inhibitor-treated-*A. phagocytophilum* tick cells when compared to the burden noted in mock-treated controls support this notion. Even though SHP-2 localizes near the intracellular surface of the cell[35,36], this molecule can be recruited to the plasma membrane by binding to tyrosine phosphorylated proteins[36]. The two SH2 domains on SHP-2 are used to interact with the tyrosine residue at the protein's active site (449Y) to make it inactive[35]. We believe arthropod SHP-2 could perform a similar role(s) in tick cells. SHP-2 interacts with receptor tyrosine kinases (RTK) and can inhibit signal transduction through phosphorylation of the tyrosine residue on the RTK[35]. When SHP-2 is inhibited, the activity of RTKs is increased. RTKs will then activate MAPK signaling[43]. We have previously reported that *A. phagocytophilum* requires p38-MAPK for its infection in tick cells[18]. We believe that upon knockdown of *shp-2* gene expression or functional inhibition of SHP-2, the RTKs activate MAPK signaling, including p38 MAPK, that could eventually contribute to increased *A. phagocytophilum* burden in tick cells.

SHP-2 is an upstream molecular player in mTOR signaling[33,36]. The data from immunoblotting analysis with knockdown of *shp-2* gene expression or functional inhibition of SHP-2 that affect mTOR activation support similar order of these molecules in the signaling cascade in ticks. We also believe that just like SHP-2 expression, the upregulation of mTOR transcripts upon *A. phagocytophilum* infection could also be a host response. The observation of increased bacterial loads in *mTOR*-dsRNA-treated or rapamycin-treated-*A. phagocytophilum* tick cells compared to the loads noted in mock-treated controls support this idea. In addition to its role in the inhibition of autophagy, cell survival, cell proliferation, and differentiation, mTOR also regulates immune responses, including anti-bacterial responses, in mammalian cells and lower vertebrates[36,38,44,45]. Therefore, we believe that upon *A. phagocytophilum* infection, SHP-2 induces mTOR activation in ticks. The increased activation of mTOR could induce tick innate immune responses, including anti-bacterial responses, that could limit *A. phagocytophilum* burden in tick cells.

Rapamycin is a chemical compound that interacts with mTOR[37,38]. This is accomplished through its binding with peptidyl-propyl-isomerase FKBP12 and then directly binding to mTOR, leading to its inhibition[37,38]. The effect of rapamycin on tick cells shows a similar phenomenon of this compound in mammalian cells. The inhibition of mTOR leads to a decrease in cellular growth and an increase in autophagy activity. Certain proteins such as ATG13, ULK1, ATG14, beclin-1, and p300 are responsible for the initiation, nucleation, and elongation of the autophagosome[38]. mTOR regulation impacts autophagosome growth through its interactions with certain autophagy-related proteins[38]. The observation of unaltered levels of all tested autophagy gene transcripts upon treatment of tick cells with rapamycin suggests that regulation of autophagy genes upon *A. phagocytophilum* is independent of the mTOR signaling. Previous reports indicated that *A. phagocytophilum* requires several autophagy molecules for the formation

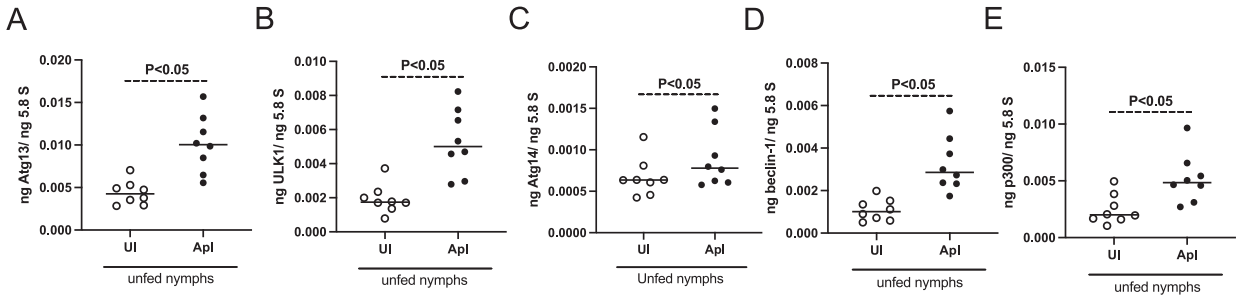

Fig. 5 | Autophagy molecules are upregulated upon *A. phagocytophilum* infection in ticks. QRT-PCR analysis showing transcript levels of *atg13* (**A**), *ulk1* (**B**), *atg14* (**C**), *beclin-1* (**D**), and *p300* (**E**) in uninfected (UI) and *A. phagocytophilum*-infected (ApI) unfed nymphal ticks. In all panels, open circles represent data from uninfected unfed nymphal ticks and the closed circles represent data from *A. phagocytophilum*-infected unfed nymphal ticks. The transcript levels of autophagy molecules were normalized to 5.8S rRNA levels. *P* value from the non-paired *t*-test is shown.

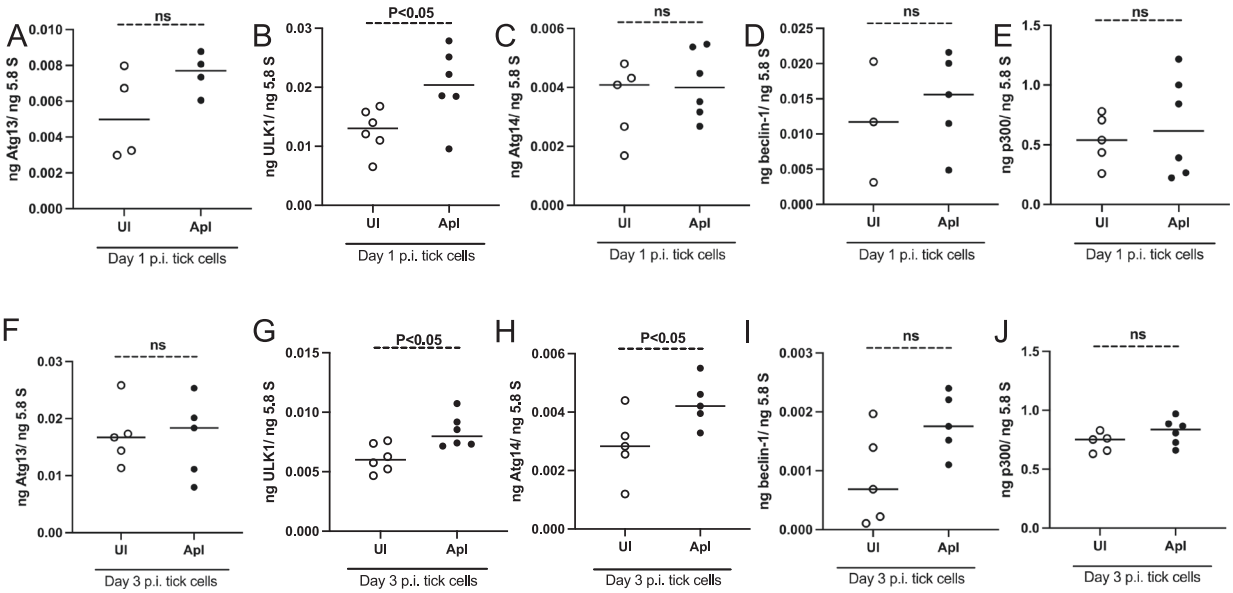

Fig. 6 | Expression of some of the autophagy molecules are altered upon *A. phagocytophilum* infection in tick cells. QRT-PCR analysis showing transcript levels of *atg13* (**A**), *ulk1* (**B**), *atg14* (**C**), *beclin-1* (**D**), and *p300* (**E**) in uninfected (UI) and *A. phagocytophilum*-infected (ApI) tick cells at days 1 (**A**–**E**) or day 3 (**F**–**J**) p.i. In all panels, open circles represent data from uninfected tick cells and the closed circles represent data from *A. phagocytophilum*-infected tick cells. The transcript levels of autophagy molecules were normalized to 5.8S rRNA levels. *P* value from the non-paired *t*-test is shown. ns indicates not significant.

of its host-derived vacuole[40]. The bacteria divide in these vacuoles[3]. In addition, treatment of mammalian cells with rapamycin increased the bacterial loads[40]. Based on the observation of rapamycin treatment in increasing bacterial loads in tick cells, we believe that *A. phagocytophilum* also subverts autophagy in tick cells for its survival. The observation of reduced *A. phagocytophilum* loads upon ATG14 or ULK1 silencing in tick cells supports this view.

In summary, our study not only provides evidence that upon *A. phagocytophilum* infection, *I. scapularis* SHP-2 and mTOR are upregulated possibly to limit the bacterial infection but also indicate that this bacterium modulates autophagy genes such as ATG14 and ULK1 for its survival in this medically important vector.

Methods

Ticks, tick cells, and bacteria

The *Ixodes scapularis* ticks used throughout the study were reared in a laboratory setting[17,18]. The ticks that were used in this study were larvae, nymphs, adult females, and adult male ticks. These ticks were obtained from BEI Resources/Center for Disease Control (CDC) or from the Oklahoma University Tick Rearing Center. *A. phagocytophilum*-infected nymphs were generated by feeding larvae on infected mice as described in our previous studies[17,18,23]. The *I. scapularis* tick cell line ISE6 was purchased from BEI Resources/ATCC (American Type Culture Collection) and maintained as described in our previous studies[17,18,22,23]. *A. phagocytophilum* isolate NCH-1 (obtained from BEI resources, USA) was used in all studies. Laboratory tick rearing was performed in an incubator set at 23 ± 2 °C with 95% humidity and a 14/10-h light/dark photoperiod regiment.

Mice studies

Tick feeding on mice was performed as in our previous studies[17,18,20,22]. Briefly, to generate uninfected, during feeding and post-fed ticks, unfed nymphal ticks were fed on uninfected or *A. phagocytophilum*-infected C57BL/6 J mice (4–6 weeks old female mice, Jackson Laboratories, USA). *A. phagocytophilum* infection was maintained in B6.129S7-Rag1tm1Mom/J ($RAG^{-/-}$) mice (4–6 weeks old female mice, Jackson Laboratories, USA). When mice are not used for tick feeding, they are housed in a group. For tick-feeding studies, mice are housed in a single cage. To generate unfed nymphs, larval ticks were fed on either uninfected or *A. phagocytophilum*-infected mice. Fully engorged repleted larval ticks were molted into unfed nymphs. For acquisition studies, *A. phagocytophilum* dense core (DC) form was isolated from 30 ml of day six infected HL-60 cells (~3.0×10^6 cells/10 ml) as described[46]. The pelleted bacteria were re-suspended in 1 ml of 1× PBS. One hundred

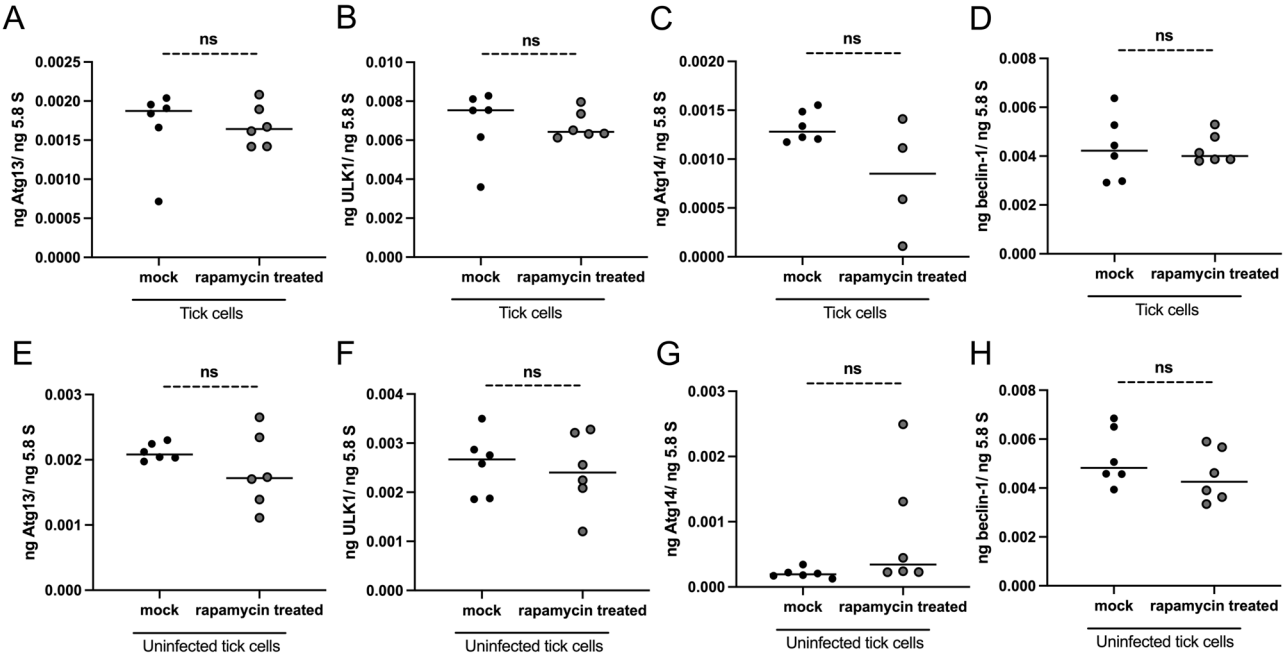

Fig. 7 | Expression of autophagy molecules was unaltered upon rapamycin treatment of *A. phagocytophilum*-infected tick cells. QRT-PCR analysis showing transcript levels of *atg13* (**A**, **E**), *ulk1* (**B**, **F**), *atg14* (**C**, **G**), and *beclin-1* (**D**, **H**) in mock- or rapamycin-treated *A. phagocytophilum*-infected (**A**–**D**) or uninfected (**E**–**H**) tick cells. Each dot represents data from the sample collected from one culture plate well. Black circles represent data from mock (DMSO)-treated, and gray circles represent data from rapamycin-treated *A. phagocytophilum*-infected (**A**–**D**) or uninfected (**E**–**H**) tick cells. The transcript levels of autophagy molecules were normalized to 5.8S rRNA levels. *P* value from the non-paired *t*-test is shown. ns indicates not significant.

microliters of this solution were injected per mouse (5 mice/group). Around 20–25 unfed nymphs were fed on each mouse. At 48 h post tick placement, intact ticks that were feeding (during feeding) were pulled off from the mice and were called 48 h during feeding nymphs. Post-feeding (PF) ticks that were repleted and were collected from 72 h to 96 h post tick placement onto the mice were called 48 h post-fed nymphs. Ticks fed on uninfected mice were used as controls. *A. phagocytophilum* infection in ticks was analyzed by Quantitative real-time PCR (QRT-PCR) as described in the relevant methods section. Unfed or during feeding or post-fed uninfected or *A. phagocytophilum*-infected nymphal ticks were processed for DNA, RNA, or protein extractions and were used for QRT-PCR analysis or immunoblotting analysis.

Ethical statement

All animal work was carried out in accordance with the regulations of the University of Tennessee, Knoxville, Institutional Care and Use of Laboratory Animals (IACUC, animal assurance number D16-00397). The IACUC approved protocol (permit # 2801–0221) was used in this study. We have complied with all relevant ethical regulations for animal use. To minimize anxiety and/or discomfort during tick feeding, mice were administered with acepromazine tranquilizer, and all efforts were made to minimize mice suffering.

DNA and RNA extractions, cDNA synthesis, and quantitative real-time PCR (QRT-PCR) analysis

Aurum total RNA mini kit (BioRad, USA) was used to isolate the DNA and RNA from the different tick developmental stages, unfed/fed ticks, and uninfected/*A. phagocytophilum*-infected ticks and tick cells, and dsRNA/inhibitor-treated tick cell samples. Total RNA isolated from samples (after DNase I treatment) was converted into cDNA using an iScript cDNA synthesis kit (BioRAD, USA), and the cDNA generated from this kit was used as a template for quantifying transcripts of *shp-2*, *mTOR*, and autophagy markers. Supplementary Table 1 shows the forward and reverse oligonucleotides used in this study. QRT-PCR was performed using CFX96 Opus QPCR machine (BioRAD, USA) and iQ-SYBR Green Supermix (BioRAD, USA) and Maxima SYBR/R (FisherThermoScientific, USA) as described[17,18,22]. To quantify the *A. phagocytophilum* bacterial burden, genomic DNA was generated from ticks and tick cell samples using a DNeasy DNA isolation kit (QIAGEN) and was processed with specific primers for PCR quantification of the *A. phagocytophilum p44* gene as reported in our previous studies with oligos shown in Supplementary Table 1[17,18,22]. The standard curves for the QRT-PCRs were made through a serial dilution of gene-specific fragments starting from 1 ng to 0.00001 ng quantities. DNA quantities were measured using a Cytation 7 reader (BioTek, USA).

Immunoblotting analysis

Immunoblotting was performed as described and with the method described in this section[17,18,23]. Briefly, total lysates from unfed or fed ticks or ISE6 tick cells were prepared in modified RIPA lysis buffer (BioExpress/VWR, USA) supplemented with an EDTA-free protease inhibitor cocktail (Sigma, USA). Tick and tick cell protein concentrations were measured using a Bradford (BCA) protein assay kit (Pierce/ThermoScientific, USA). Primary (SHP2 antibody-product number 3752S, phospho-mTOR antibody-product number 2971S) and secondary antibodies (product number 7074S) were purchased from Cell Signaling Technologies (USA). Twenty-five micrograms of total lysates were generated from uninfected/*A. phagocytophilum*-infected tick samples were loaded onto a 12% reducing SDS-PAGE gel for immunoblotting analysis. Primary antibodies were used in 1:1000 dilution and secondary antibody was used in 1:5000 dilution for 5 ml solutions. Untreated/treated tick cell samples (20 or 25 µg) were loaded onto an 8% reducing SDS-PAGE gel for immunoblotting analysis. Ponceau-S stained membrane or TCE gel images were used to indicate loading controls for the immunoblots. Blots were imaged using the ChemiDoc Imaging system (BioRAD, USA) and processed using Image Lab software (BioRAD, USA).

dsRNA synthesis and transfections

The dsRNA synthesis was performed as described[22,23,28]. The template for dsRNA synthesis was selected from the coding sequence (CDS) and the

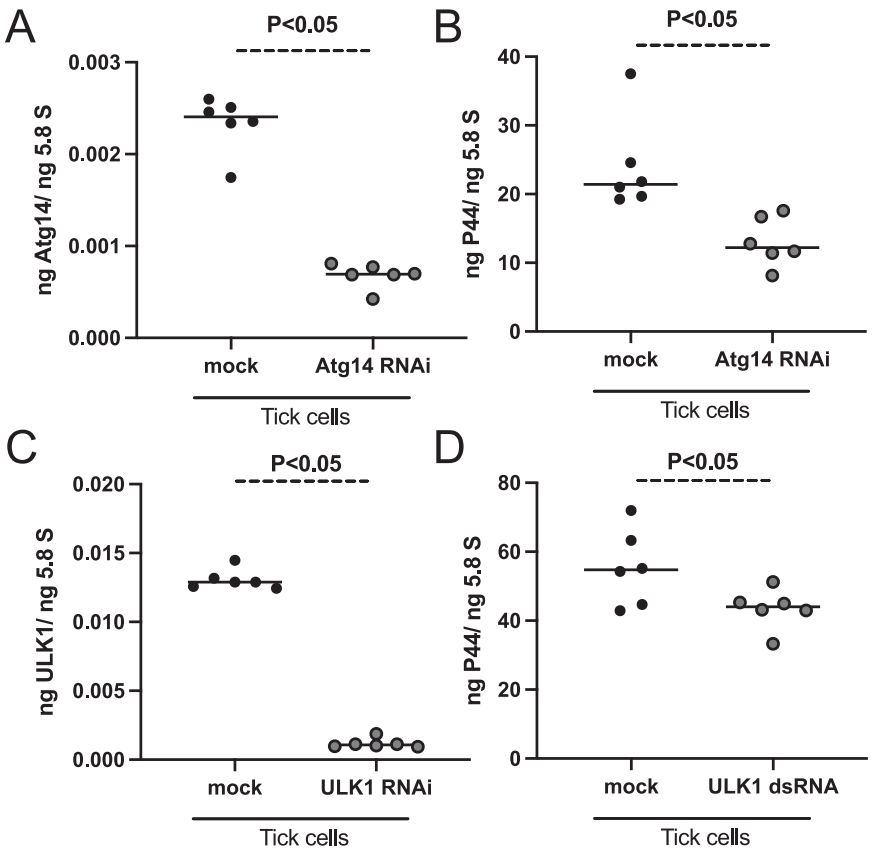

Fig. 8 | RNAi-mediated silencing of *atg14* and *ulk1* expression affects bacterial growth in tick cells. **A** QRT-PCR analysis showing the silencing efficiency of *atg14* expression (**A**) or bacterial burden (**B**) after 24-h post *A. phagocytophilum* infection in mock- or *atg14*-dsRNA-treated tick cells. **C** QRT-PCR analysis showing the silencing efficiency of *ulk1* expression (**C**) or bacterial burden (**D**) after 24-h post *A. phagocytophilum* infection in mock- or *ulk1*-dsRNA-treated tick cells. In all panels, closed black circles represent data from mock-dsRNA-treated, and gray circles represent *atg14*- (**A**, **B**) or *ulk1*-dsRNA-treated (**C**, **D**) *A. phagocytophilum*-infected tick cells. Each dot represents data from a sample collected from one independent culture plate well. The transcript levels of *atg14, ulk1*, and *p44* DNA levels were normalized to 5.8S rRNA levels. *P* value from the non-paired *t*-test is shown.

fragment was generated from cDNA. The *shp-2* gene fragment (329 bp) was PCR amplified using gene-specific primers containing BglII (forward primer) and KpnI (reverse primer) restriction enzyme sites (forward 5' CC AGATCTGAGGGAGAGCCGCAGCA 3' and the reverse 5' CGGGTA CCCCTGTTGCTGCAGGTGCTCA 3'). The *Escherichia coli* JM109 cells were used for generating the *shp2*-dsRNA clone in the pL4440 plasmid[19,47]. The pL4440 vector has two T7 promoters on either end of multiple cloning sites close to the BglII and KpnI sites. The *shp2*-fragment cloned vector was digested with BglII or KpnI separately and processed for in vitro transcription. The *ulk1* gene fragment (414 bp) was PCR amplified using gene-specific primers with T7 promoter (forward 5' GCTAATACGACTC ACTATAGGGAGAGCCAAGGGCATAGTGCACA 3' and reverse 5' GCTAATACGACTCACTATAGGGAGAGTCCATCCTCTCTCTTGCA TTCT 3'). The *atg14* gene fragment (503 bp) was PCR amplified using gene-specific primers with T7 promoters (forward 5' GCTAATACGACTCA CTATAGGGAGAGCGACTTCACCAGCTCCA 3' and reverse 5' GCTAA TACGACTCACTATAGGGAGACCAGACGTCGTCCTCCTGA 3'). As *ulk1* or *atg14* PCR fragments contain T7 promoters, they were directly processed for in vitro transcription. The dsRNA that was complementary to the *shp2*, *ulk1*, and *atg14* fragments was generated using the MEGAscript RNAi Kit (Ambion Inc., USA) and by following the manufacturer's instructions.

ISE6 tick cells and lipofectamine (3 µl/1 ml culture) reagent (Invitrogen/ThermoFisher Scientific Inc., USA) were used for the transfection experiments. For each well, 1.0×10^5 ISE6 tick cells were seeded in L-15B300 medium onto 12 well plates and incubated overnight for 18–20 h. After cell attachment and spreading, 750 ng of dsRNA was added with lipofectamine reagent into each well. There were six replicates for each group on the 12 well plate and the ISE6 tick cells were incubated for 5 h after treatment, then 1 ml of 2× L15-B300 medium was added to each of the wells. The 12-well plate was then incubated for another 18–20 h. A human promyelocytic cell line (HL-60 cells, obtained from ATCC, USA) was used to maintain *A. phagocytophilum* NCH1. Cell-free *A. phagocytophilum* was isolated from infected HL-60 cells as described in refs. 18,23. Cell-free bacteria isolated from these cells were used for in vitro infection studies. *A. phagocytophilum* infection was performed 24 h post-transfection and the plate was incubated for an additional 24 h then ISE6 tick cell samples were collected and processed for RNA and DNA extractions. Silencing efficiency and bacterial burden were determined by QRT-PCR analysis of the RNA or DNA samples, respectively. Cell viability was tested by microscopic examination and MTT assays as shown in Supplementary Figs. 6 and 11. MTT assays were performed as described ref. 17.

Inhibitor studies

The SHP-2 inhibitor (JAB-3068) was purchased from ChemieTek (CT, USA) and it is a PTP type 11 inhibitor. The mTOR inhibition was done with Rapamycin as it targets the mTOR protein's active site. Concentrated stocks (500 µM) of SHP-2 inhibitor or Rapamycin were prepared in a DMSO solution. Mock tick cell samples had an equivalent amount of DMSO added to each of the wells, corresponding to the inhibitor used in that experiment. ISE6 tick cells (1.0×10^5 cells per well) were seeded onto a 12-well plate and incubated for 18–20 h and each group had six replicates. After incubation, the cells were treated with either SHP-2 inhibitor Rapamycin, or mock solution. The final concentration of SHP-2 inhibitor in each of the treated wells was 25 µM and the final concentration of Rapamycin in each of the treated wells was 1.1 µM. After 4 h of treatment, the mock or inhibitor-treated wells were infected with *A. phagocytophilum* and incubated for an additional 24 h. The ISE6 tick cell samples were then collected and processed for RNA and DNA extractions to measure *shp-2* or *mTOR* transcripts and the bacterial burden.

Statistics and reproducibility

Prism6 software and Microsoft Excel 2019 were used for performing statistical analysis in the data sets. Scatter plot graphs were generated in Prism6 software. Each open or closed circle, square, triangle, and inverted triangle in the Scatter plot graphs represents one data point generated from

the average of two technical replicates. Sample sizes in each graph can be determined based on the number of data points seen in each Scatter plot graph and it ranges from three to eight per group. When comparing two means, an unpaired, two-tailed, *t*-test was performed. *P* values less than 0.05 were considered significant and *P* values greater than 0.05 were considered not significant in each of the analyses. Wherever necessary *P* values are indicated. ANOVA analysis was used to obtain *P* values when more than two groups were compared.

GenBank accession numbers

The GenBank accession numbers used and analyzed in this study are shown in Supplementary Table 2.

Reporting summary

Further information on research design is available in the Nature Portfolio Reporting Summary linked to this article.

Data availability

All data generated or analyzed during this study are included in the main manuscript or supplementary file. Full-length uncropped blots are shown in the main figures. Source data for graphs are included as a Supplementary data file. Full-length blot for Fig. 1G is shown in Supplementary Fig. 13. Full-length blots for Fig. 4C, D, and E are shown in Supplementary Fig. 14. Supplementary Fig. 7 contains full-length agarose gel image showing amplification of mTOR transcript fragment from unfed tick nymphs.

Received: 16 August 2024; Accepted: 28 February 2025;
Published online: 13 March 2025

References

1. Hodzic, E. et al. Acquisition and transmission of the agent of human granulocytic ehrlichiosis by Ixodes scapularis ticks. *J. Clin. Microbiol.* **36**, 3574–3578 (1998).
2. Richter, P. J. et al. Ixodes pacificus (Acari: Ixodidae) as a vector of *Ehrlichia equi* (Rickettsiales: Ehrlichieae). *J. Med. Entomol.* **33**, 1–5 (1996).
3. Rikihisa, Y. Mechanisms of obligatory intracellular infection with *Anaplasma phagocytophilum*. *Clin. Microbiol. Rev.* **24**, 469–489 (2011).
4. Kocan, K. M., de la Fuente, J. & Cabezas-Cruz, A. The genus anaplasma: new challenges after reclassification. *Rev. Sci. Tech.* **34**, 577–586 (2015).
5. Anderson, J. F. & Magnarelli, L. A. Biology of ticks. *Infect. Dis. Clin. North Am.* **22**, 195–215 (2008).
6. de la Fuente, J., Estrada-Pena, A., Venzal, J. M., Kocan, K. M. & Sonenshine, D. E. Overview: ticks as vectors of pathogens that cause disease in humans and animals. *Front. Biosci. Landmrk* **13**, 6938–6946 (2008).
7. Bakken, J. S. & Dumler, J. S. Human granulocytic anaplasmosis. *Infect. Dis. Clin. North Am.* **29**, 341–355 (2015).
8. Carlyon, J. A. & Fikrig, E. Invasion and survival strategies of *Anaplasma phagocytophilum*. *Cell Microbiol.* **5**, 743–754 (2003).
9. Chen, S. M., Dumler, J. S., Bakken, J. S. & Walker, D. H. Identification of a granulocytotropic ehrlichia species as the etiologic agent of human-disease. *J. Clin. Microbiol.* **32**, 589–595 (1994).
10. Munderloh, U. G. et al. Invasion and intracellular development of the human granulocytic ehrlichiosis agent in tick cell culture. *J. Clin. Microbiol.* **37**, 2518–2524 (1999).
11. Carlyon, J. A., Abdel-Latif, D., Pypaert, M., Lacy, P. & Fikrig, E. *Anaplasma phagocytophilum* utilizes multiple host evasion mechanisms to thwart NADPH oxidase-mediated killing during neutrophil infection. *Infect. Immun.* **72**, 4772–4783 (2004).
12. Ge, Y. & Rikihisa, Y. *Anaplasma phagocytophilum* delays spontaneous human neutrophil apoptosis by modulation of multiple apoptotic pathways. *Cell Microbiol.* **8**, 1406–1416 (2006).
13. Truchan, H. K., Cockburn, C. L., May, L. J., VieBrock, L. & Carlyon, J. A. *Anaplasma phagocytophilum*-occupied vacuole interactions with the host cell cytoskeleton. *Vet Sci.* https://doi.org/10.3390/vetsci3030025 (2016).
14. Garcia-Garcia, J. C., Barat, N. C., Trembley, S. J. & Dumler, J. S. Epigenetic silencing of host cell defense genes enhances intracellular survival of the rickettsial pathogen *Anaplasma phagocytophilum*. *PLoS Pathog.* **5**, e1000488 (2009).
15. Niu, H., Xiong, Q., Yamamoto, A., Hayashi-Nishino, M. & Rikihisa, Y. Autophagosomes induced by a bacterial Beclin 1 binding protein facilitate obligatory intracellular infection. *Proc. Natl. Acad. Sci. USA* **109**, 20800–20807 (2012).
16. Khanal, S., Taank, V., Anderson, J. F., Sultana, H. & Neelakanta, G. Arthropod transcriptional activator protein-1 (AP-1) aids tick-rickettsial pathogen survival in the cold. *Sci. Rep.* **8**, 11409 (2018).
17. Mahesh, P. P., Namjoshi, P., Sultana, H. & Neelakanta, G. Immunization against arthropod protein impairs transmission of rickettsial pathogen from ticks to the vertebrate host. *NPJ Vaccines* **8**, 79 (2023).
18. Namjoshi, P., Dahmani, M., Sultana, H. & Neelakanta, G. Rickettsial pathogen inhibits tick cell death through tryptophan metabolite mediated activation of p38 MAP kinase. *iScience* **26**, 105730 (2023).
19. Neelakanta, G., Sultana, H., Fish, D., Anderson, J. F. & Fikrig, E. *Anaplasma phagocytophilum* induces Ixodes scapularis ticks to express an antifreeze glycoprotein gene that enhances their survival in the cold. *J. Clin. Invest.* **120**, 3179–3190 (2010).
20. Ramasamy, E., Taank, V., Anderson, J. F., Sultana, H. & Neelakanta, G. Repression of tick microRNA-133 induces organic anion transporting polypeptide expression critical for *Anaplasma phagocytophilum* survival in the vector and transmission to the vertebrate host. *PLoS Genet.* **16**, e1008856 (2020).
21. Sultana, H. et al. Anaplasma phagocytophilum induces actin phosphorylation to selectively regulate gene transcription in Ixodes scapularis ticks. *J. Exp. Med.* **207**, 1727–1743 (2010).
22. Taank, V. et al. Human rickettsial pathogen modulates arthropod organic anion transporting polypeptide and tryptophan pathway for its survival in ticks. *Sci. Rep.* **7**, 13256 (2017).
23. Turck, J. W., Taank, V., Neelakanta, G. & Sultana, H. Ixodes scapularis Src tyrosine kinase facilitates *Anaplasma phagocytophilum* survival in its arthropod vector. *Ticks Tick. Borne Dis.* **10**, 838–847 (2019).
24. Alberdi, P., Espinosa, P. J., Cabezas-Cruz, A. & de la Fuente, J. *Anaplasma phagocytophilum* manipulates host cell apoptosis by different mechanisms to establish infection. *Vet Sci*. https://doi.org/10.3390/vetsci3030015 (2016).
25. McClure Carroll, E. E. et al. p47 licenses activation of the immune deficiency pathway in the tick Ixodes scapularis. *Proc. Natl. Acad. Sci. USA* **116**, 205–210 (2019).
26. Ayllon, N. et al. *Anaplasma phagocytophilum* inhibits apoptosis and promotes cytoskeleton rearrangement for infection of tick cells. *Infect. Immun.* **81**, 2415–2425 (2013).
27. Artigas-Jeronimo, S. et al. *Anaplasma phagocytophilum* modifies tick cell microRNA expression and upregulates isc-mir-79 to facilitate infection by targeting the roundabout protein 2 pathway. *Sci. Rep.* **9**, 9073 (2019).
28. Khanal, S., Taank, V., Anderson, J. F., Sultana, H. & Neelakanta, G. Rickettsial pathogen perturbs tick circadian gene to infect the vertebrate host. *Int. J. Mol. Sci*. https://doi.org/10.3390/ijms23073545 (2022).
29. Cabezas-Cruz, A., Espinosa, P., Alberdi, P. & de la Fuente, J. Tick-pathogen interactions: the metabolic perspective. *Trends Parasitol.* **35**, 316–328 (2019).
30. Bononi, A. et al. Protein kinases and phosphatases in the control of cell fate. *Enzym. Res.* **2011**, 329098 (2011).

31. Thomas, V. & Fikrig, E. *Anaplasma phagocytophilum* specifically induces tyrosine phosphorylation of ROCK1 during infection. *Cell Microbiol.* **9**, 1730–1737 (2007).
32. Lin, M. Q., den Dulk-Ras, A., Hooykaas, P. J. J. & Rikihisa, Y. *Anaplasma phagocytophilum* AnkA secreted by type IV secretion system is tyrosine phosphorylated by Abl-1 to facilitate infection. *Cell. Microbiol.* **9**, 2644–2657 (2007).
33. Niogret, C., Birchmeier, W. & Guarda, G. SHP-2 in lymphocytes' cytokine and inhibitory receptor signaling. *Front Immunol.* **10**, 2468 (2019).
34. Wu, C. J. et al. The tyrosine phosphatase SHP-2 is required for mediating phosphatidylinositol 3-kinase/Akt activation by growth factors. *Oncogene* **20**, 6018–6025 (2001).
35. Jarvis, L. A., Toering, S. J., Simon, M. A., Krasnow, M. A. & Smith-Bolton, R. K. Sprouty proteins are in vivo targets of Corkscrew/SHP-2 tyrosine phosphatases. *Development* **133**, 1133–1142 (2006).
36. Feng, G. S. Shp-2 tyrosine phosphatase: signaling one cell or many. *Exp. Cell Res.* **253**, 47–54 (1999).
37. Saxton, R. A. & Sabatini, D. M. mTOR signaling in growth, metabolism, and disease. *Cell* **169**, 361–371 (2017).
38. Dossou, A. S. & Basu, A. The emerging roles of mTORC1 in macromanaging autophagy. *Cancers*. https://doi.org/10.3390/cancers11101422 (2019).
39. Ijdo, J. W., Carlson, A. C. & Kennedy, E. L. AnkA is tyrosine-phosphorylated at EPIYA motifs and recruits SHP-1 during early infection. *Cell. Microbiol.* **9**, 1284–1296 (2007).
40. Niu, H., Yamaguchi, M. & Rikihisa, Y. Subversion of cellular autophagy by *Anaplasma phagocytophilum*. *Cell Microbiol.* **10**, 593–605 (2008).
41. Bonne Kohler, J. et al. Importance of protein Ser/Thr/Tyr phosphorylation for bacterial pathogenesis. *FEBS Lett.* **594**, 2339–2369 (2020).
42. DeVinney, R., Steele-Mortimer, O. & Finlay, B. B. Phosphatases and kinases delivered to the host cell by bacterial pathogens. *Trends Microbiol.* **8**, 29–33 (2000).
43. Regad, T. Targeting RTK signaling pathways in cancer. *Cancers* **7**, 1758–1784 (2015).
44. Li, K., Wei, X. M., Zhang, L. B., Chi, H. & Yang, J. L. Raptor/mTORC1 acts as a modulatory center to regulate anti-bacterial immune response in rockfish. *Front Immunol.* **10**, ARTN 2953 (2019).
45. Weichhart, T. et al. The TSC-mTOR signaling pathway regulates the innate inflammatory response. *Immunity* **29**, 565–577 (2008).
46. Taank, V., Ramasamy, E., Sultana, H. & Neelakanta, G. An efficient microinjection method to generate human anaplasmosis agent *Anaplasma phagocytophilum*-infected ticks. *Sci. Rep.* **10**, 15994 (2020).
47. Narasimhan, S. et al. Disruption of Ixodes scapularis anticoagulation by using RNA interference. *Proc. Natl. Acad. Sci. USA* **101**, 1141–1146 (2004).

Acknowledgements

The following reagents were provided by Centers for Disease Control and Prevention for distribution by BEI Resources, NIAID, NIH: *Ixodes scapularis* Adult (Live), NR-42510, Larvae (Live), NR-44115 and Nymph (Live), NR-44116. This study was supported in part by funding from the National Institute of Allergy and Infectious Diseases (NIAID), the National Institutes of Health (NIH) (award number: R01AI130116) to G.N. and the University of Tennessee, Knoxville Start-up funds to H.S. and G.N.

Author contributions

J.W.T. performed the experiments. G.N. helped with the animal experiments. J.W.T., H.S., and G.N. analyzed and interpreted the data. J.W.T., H.S., and G.N. designed the study. H.S. and G.N. provided reagents. All authors read, edited, and approved the manuscript. J.W.T. and G.N. wrote the paper. G.N. conceptualized and conceived the study and supervised overall investigations.

Competing interests

The authors declare that they have no conflicts of interest with the contents of this article.

Additional information

Supplementary information The online version contains supplementary material available at https://doi.org/10.1038/s42003-025-07859-6.

Correspondence and requests for materials should be addressed to Girish Neelakanta.

Peer review information *Communications Biology* thanks Hema Narra, Deepika Chauhan, and Latre De Late Perle for their contribution to the peer review of this work. Primary Handling Editors: Karthika Rajeeve and David Favero.

Reprints and permissions information is available at http://www.nature.com/reprints

Publisher's note Springer Nature remains neutral with regard to jurisdictional claims in published maps and institutional affiliations.

Open Access This article is licensed under a Creative Commons Attribution-NonCommercial-NoDerivatives 4.0 International License, which permits any non-commercial use, sharing, distribution and reproduction in any medium or format, as long as you give appropriate credit to the original author(s) and the source, provide a link to the Creative Commons licence, and indicate if you modified the licensed material. You do not have permission under this licence to share adapted material derived from this article or parts of it. The images or other third party material in this article are included in the article's Creative Commons licence, unless indicated otherwise in a credit line to the material. If material is not included in the article's Creative Commons licence and your intended use is not permitted by statutory regulation or exceeds the permitted use, you will need to obtain permission directly from the copyright holder. To view a copy of this licence, visit http://creativecommons.org/licenses/by-nc-nd/4.0/.

© The Author(s) 2025